

Multirate Neural Image Compression with Adaptive Lattice Vector Quantization

Supplementary Material

1. Additional R-D curves

In Figs. 1 to 3, we present R-D curves for the three architectures: Cheng2020 architecture [1], Cheng2020 Checkerboard architecture [2] and MBT2018 mean architecture [3], evaluated on the Tecnick dataset. We also present R-D curves for the Cheng2020 checkerboard [2] and MBT2018 mean [3] architectures evaluated on the Kodak and CLIC datasets in Fig. 4 and Fig. 5, which were omitted from the main text due to the page limitation.

These presented R-D curves, like those in the main text, demonstrate that our LVQ-based variable rate compression methods perform comparably to non-variable rate compression models, which require separate training for each R-D trade-off. Furthermore, the proposed LVQ-based variable rate compression models consistently outperform their SQ-based counterparts, especially at low bitrates.

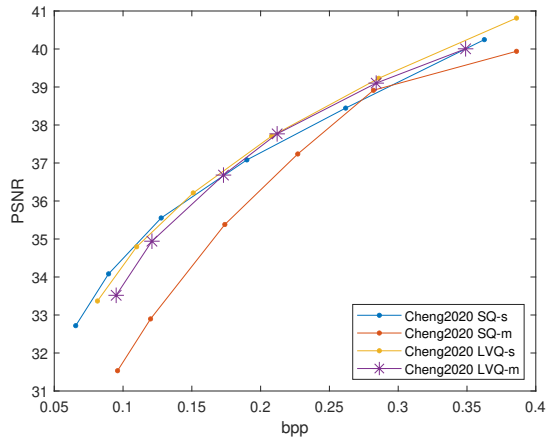


Figure 1. R-D curves for the Cheng2020 architecture [1] tested on the Tecnick dataset. Here, 'm' denotes that this model can handle multiple R-D trade-offs, while 's' indicates that this model trains separate models for each R-D trade-off.

2. Visual Comparison

Figure 6 to Fig. 11 present visual comparisons for the Cheng2020 architecture, clearly demonstrating the superiority of our proposed LVQ-based variable rate compression model over its SQ-based counterpart. At similar bitrates, the LVQ-based model achieves significantly higher PSNR values and effectively suppresses compression artifacts.

References

[1] Zhengxue Cheng, Heming Sun, Masaru Takeuchi, and Jiro Katto. Learned image compression with discretized gaussian

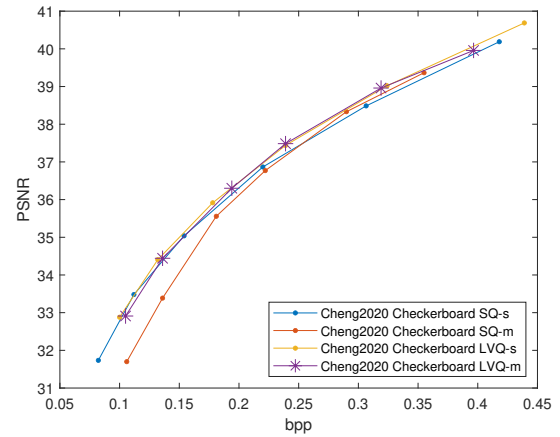


Figure 2. R-D curves for the Cheng2020 Checkerboard architecture [2] tested on the Tecnick dataset. Here, 'm' denotes that this model can handle multiple R-D trade-offs, while 's' indicates that this model trains separate models for each R-D trade-off.

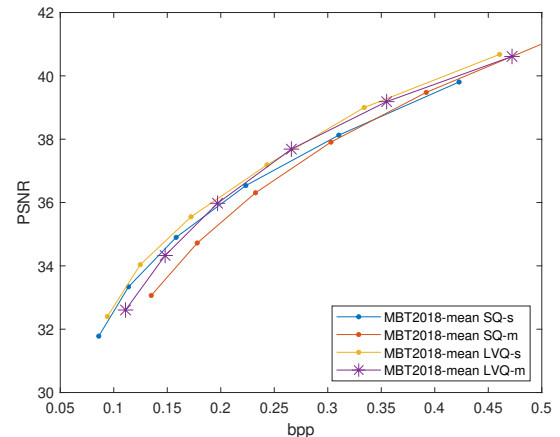
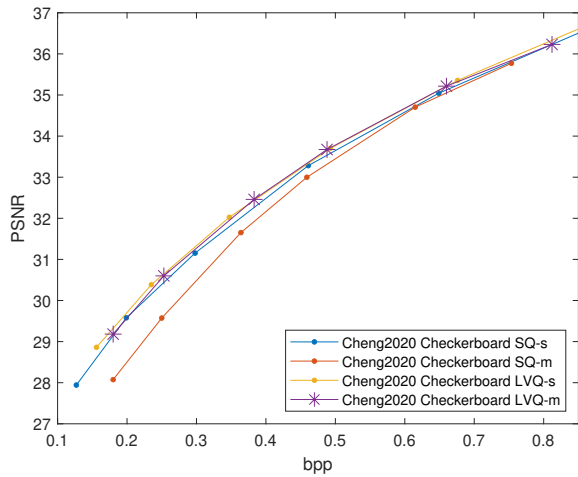


Figure 3. R-D curves for the MBT2018 mean architecture [3] tested on the Tecnick dataset. Here, 'm' denotes that this model can handle multiple R-D trade-offs, while 's' indicates that this model trains separate models for each R-D trade-off.

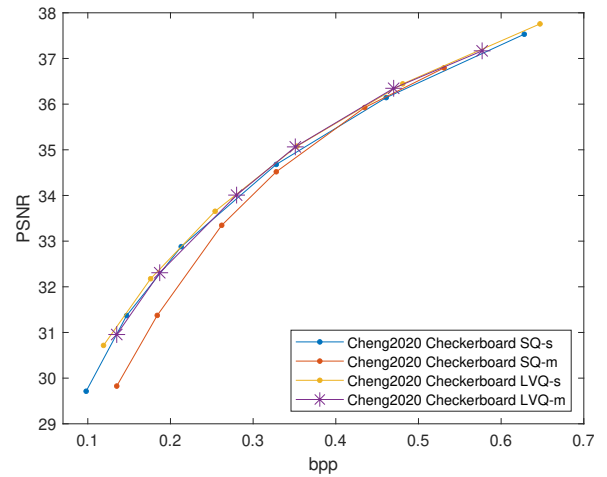
mixture likelihoods and attention modules. In *Proceedings of the IEEE/CVF conference on computer vision and pattern recognition*, pages 7939–7948, 2020. 1

[2] Dailan He, Yaoyan Zheng, Baocheng Sun, Yan Wang, and Hongwei Qin. Checkerboard context model for efficient learned image compression. In *Proceedings of the IEEE/CVF Conference on Computer Vision and Pattern Recognition*, pages 14771–14780, 2021. 1, 2

[3] David Minnen, Johannes Ballé, and George D Toderici. Joint autoregressive and hierarchical priors for learned image compression. *Advances in neural information processing systems*,

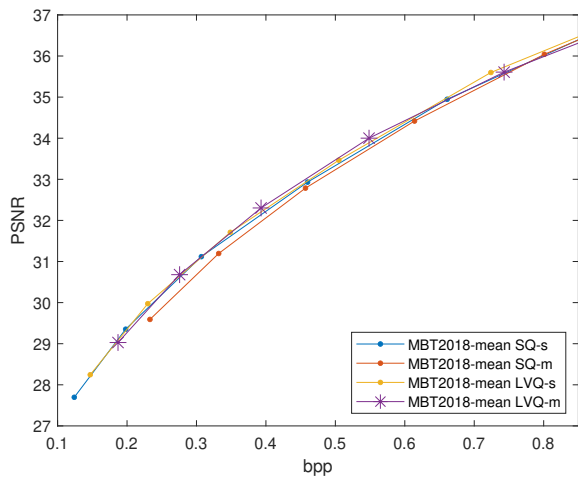


(a) Kodak

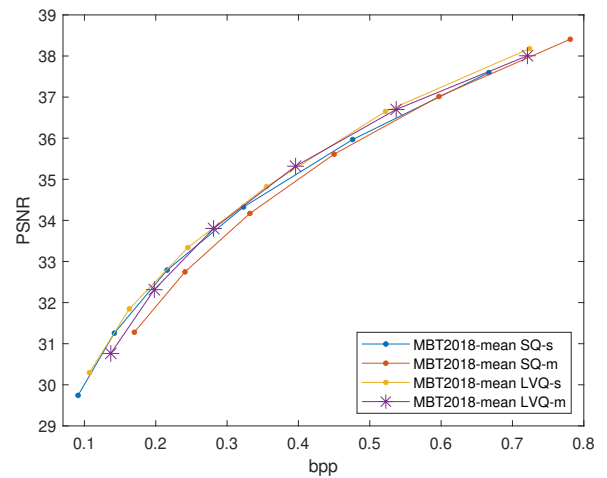


(b) CLIC validation set

Figure 4. R-D curves of for the Cheng2020 Checkerboard architecture [2] evaluated on the Kodak and CLIC datasets. Here, 'm' denotes that this model can handle multiple R-D trade-offs, while 's' indicates that this model trains separate models for each R-D trade-off.



(a) Kodak



(b) CLIC validation set

Figure 5. R-D curves of for the MBT2018 mean architecture [3] evaluated on the Kodak and CLIC datasets. Here, 'm' denotes that this model can handle multiple R-D trade-offs, while 's' indicates that this model trains separate models for each R-D trade-off.



SQ-based variable rate compression model
0.096 bpp
29.710 dB



LVQ-based variable rate compression model
0.103bpp
30.484 dB



Ground Truth

Figure 6. Visual comparisons of different variable rate compression models on 'kodim04.png' from Kodak dataset.



SQ-based variable rate compression model
0.101 bpp
30.352 dB



LVQ-based variable rate compression model
0.105 bpp
31.356 dB



Ground Truth

Figure 7. Visual comparisons of different variable rate compression models on 'kodim10.png' from Kodak dataset.



(a) SQ-based variable rate compression model, 0.075 bpp, 30.926 dB



(b) LVQ-based variable rate compression model, 0.078 bpp, 32.169 dB



(c) Ground Truth

Figure 8. Visual comparisons of different variable rate compression models on 'kodim03.png' from Kodak dataset.



(a) SQ-based variable rate compression model, 0.181 bpp, 27.822 dB



(b) LVQ-based variable rate compression model, 0.190 bpp, 28.141 dB



(c) Ground Truth

Figure 9. Visual comparisons of different variable rate compression models on 'kodim06.png' from Kodak dataset.



(a) SQ-based variable rate compression model, 0.073 bpp, 30.517 dB



(b) LVQ-based variable rate compression model, 0.080 bpp, 31.562 dB



(c) Ground Truth

Figure 10. Visual comparisons of different variable rate compression models on 'kodim12.png' from Kodak dataset.



(a) SQ-based variable rate compression model, 0.105 bpp, 28.831 dB



(b) LVQ-based variable rate compression model, 0.095 bpp, 31.421 dB



(c) Ground Truth

Figure 11. Visual comparisons of different variable rate compression models on 'kodim20.png' from Kodak dataset.